

Decoherence and the Reemergence of Coherence From a Superconducting “Horizon”

Eric J. Sung^{✉*}

Program in Applied Mathematics, University of Arizona, Tucson, AZ 85721, USA

Charles A. Stafford^{✉†}

Department of Physics, University of Arizona, Tucson, AZ 85721, USA

(Dated: March 18, 2026)

In a recent paper [1], Danielson et al. demonstrated that the mere presence of a black hole causes universal decoherence of quantum superpositions (dubbed the DSW decoherence). This result has profound implications for the interplay of quantum mechanics and gravity. We analyze decoherence in a superconducting analogue [2] of the event horizon of a black hole, where Andreev reflection plays the role of Hawking radiation. We consider a normal metal interferometer threaded by an Aharonov-Bohm flux, where one of the arms of the interferometer is coupled to a superconductor by a tunnel coupling of varying strength. At absolute zero and for weak coupling, we find that the scattering states of the interferometer are decohered by Andreev reflection, a nontrivial manifestation of the proximity effect analogous to DSW decoherence from the event horizon of a black hole. However, for increasing coupling strength to the superconductor, we find a reemergence of coherence via resonant tunneling through Andreev bound states. This suggests the existence of an analogue gravitational phenomenon wherein transmission mediated by virtual Hawking radiation leads to a reemergence of coherence in an interferometer placed within a few Compton wavelengths of a black hole’s event horizon. Our results open a new path to study black hole quantum physics on earth via analogue studies.

Introduction—Physical analogies can reveal that the same mathematical structures and emergent phenomena can arise in systems with very different microscopic origins. This idea has seen popularity in analogue gravity [3], where condensed matter and quantum optical platforms reproduce hallmark features of curved spacetime physics, such as effective horizons [4–7] and Hawking-like radiation [8, 9]. Following the discovery of the Unruh effect [10–12], Unruh derived its sonic analogue [4, 5], one of the earliest analogue gravity systems. Since then, a multitude of different systems have been proposed as analogue gravity testbeds, including fermionic and bosonic superfluids [6, 13–16], Weyl and Dirac materials [7, 17], and interacting bosons on optical lattices [18]. Some of these analogue platforms have also seen experimental confirmation such as analogue Hawking radiation using Bose-Einstein condensates [19–22], optical analogues [23, 24], and superconducting circuits [25].

In this Letter, we explore the deep analogy of BCS superconductors [26] and black holes [2, 27, 28]. More specifically, we identify the solid-state analogue of the newly discovered Danielson, Satishchandran, and Wald (DSW) decoherence for black holes [1, 29, 30] in a superconductor-normal metal (SN) Aharonov-Bohm (AB) interferometer. We show that weak coupling to the SN interface suppresses interference through Andreev-induced decoherence, while intermediate coupling leads to a reemergence of coherence via resonant Andreev processes. These results demonstrate the one-to-one conceptual mapping between superconductors and black holes,

opening the possibility of utilizing superconducting interferometers as platforms for studying horizon-induced decoherence in laboratories.

Solid-State DSW Experiment—We begin with a brief description and analysis of the original DSW thought experiment. Alice prepares a spatial superposition of electrically charged particles outside a black hole and Bob is inside the black hole [1]. The superimposed matter creates superimposed electromagnetic and gravitational fields which travel into the black hole where Bob is able to measure the fields and learn about the superposition. This disturbs the superposition but by causality, Bob’s actions cannot have an effect on the superposition. Since he is, in principle, able to make such a measurement, the resolution of this paradox is that Alice’s state must disturb itself.

This thought experiment implies that from Bob’s point of view, decoherence is due to the event horizon (or more generally, a Killing horizon [29]) harvesting the which-path information of Alice’s interferometer [1, 31]. This relativistic point of view demonstrates that the space-time curvature plays a key role in decoherence. However, there exists a complementary *local* description from Alice’s point of view [30] where decoherence is mediated by low frequency Hawking radiation [8, 9]. This alternative description is interesting from the lens of analogue studies because superconductors have been noted to be black hole analogues [2, 28] in superconductor-normal metal systems [32] with the normal metal being the analogue of the exterior of the black hole. In addition, Andreev reflection [33–37], the process where an electron (hole) mode is absorbed as a Cooper pair and a hole (electron) is retro-reflected, has been noted as the analogue of Hawking radiation [27].

* jsung1@arizona.edu

† stafforc@arizona.edu

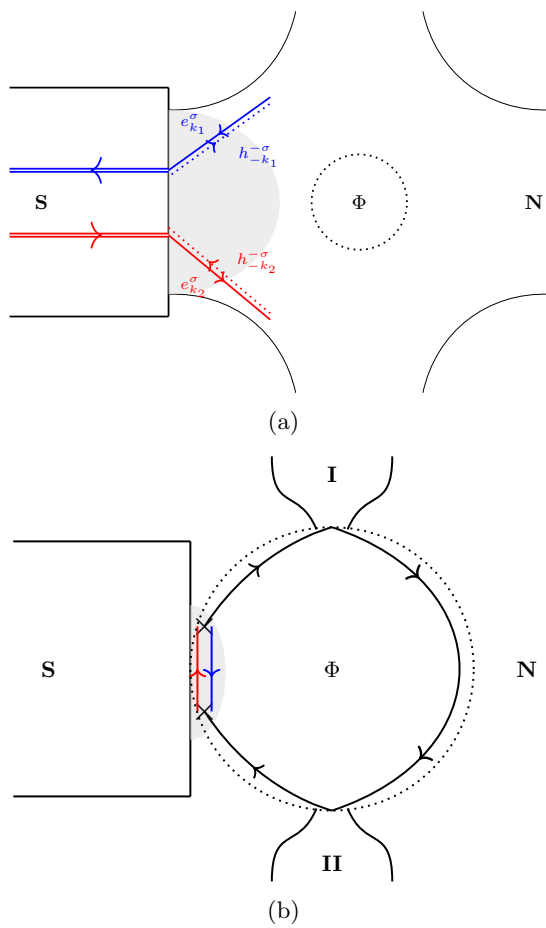


FIG. 1. Schematic diagram of a normal metal interferometer threaded by an AB flux Φ (dotted circle), coupled to a superconductor. (a) For weak coupling to the superconductor, Andreev scattering leads to decoherence in the interferometer. (b) For intermediate coupling to the superconductor, resonant tunneling through Andreev bound states causes a reemergence of coherence.

This conceptual one-to-one mapping naturally leads us to consider Alice's point of view and explore the solid-state DSW (SS-DSW) decoherence. Thus, we present the SS-DSW thought experiment: Consider a SN system with a BCS superconductor [26]. Alice is in N while Bob is deep inside S, which is kept at a temperature $T \ll \Delta(\mathbf{x})/k_B$ where $\Delta(\mathbf{x}) = \Delta_0 e^{i\phi_S(\mathbf{x})}$ is the superconducting gap with superconducting phase $\phi_S(\mathbf{x})$. Alice performs a scattering experiment using an Aharonov-Bohm interferometer [38–40] in N. An electron wave incident from a source lead is coherently split between the two arms of the interferometer, one of which is coupled to the SN interface. The outgoing transmission is measured at a drain lead through its flux-dependent interference contrast. For subgap energies $E \ll \Delta(\mathbf{x})$, the branch coupled to S can undergo Andreev conversion, thereby leaving the superconducting sector in a branch-

dependent many-body state. In contrast, the branch that does not couple to S leaves the condensate in its ground state $|\Omega\rangle_S$. Moreover, for subgap energies $E \ll \Delta(\mathbf{x})$ there are no propagating quasiparticles in S, and thermal above-gap $E > \Delta(\mathbf{x})$ quasiparticles are frozen out by $T \ll \Delta(\mathbf{x})/k_B$. Thus, which-path information deposited in S cannot be returned to Alice. Since Bob could, in principle, act on the superconducting sector and affect Alice's interference signal, we reach the inevitable conclusion that Alice's reduced state must already be disturbed by those inaccessible superconducting degrees of freedom. This is the solid-state DSW decoherence.

Interferometer Model and Decoherence Metrics—To rigorously analyze our SS-DSW thought experiment, we first consider a N -site tight-binding ring threaded by an AB flux Φ (Peierls phase $\phi = e\Phi/\hbar$). Coupled directly to the left side of the ring as a perturbation is a BCS superconductor with (uniform) order parameter Δ and coupling constant g . This effectively creates a (modified) SN system [32] (see Fig. 1b). There are two leads, $\Gamma^{I,II}$, in the wide-band limit coupled to the N -ring with coupling strength $\gamma^{I,II}$ that act as a source (lead I) and drain (lead II). An electron is inserted into the ring via lead I, traverses either path of the interferometer, then is absorbed into lead II. Depending on the SN coupling strength t_{AR} , the electron can take a detour into S and undergo Andreev reflection at the SN interface, converting into a retro-reflected hole in the process. An uncorrelated hole can then be converted into an electron that is transmitted into the drain electrode, leading to decoherence (see Fig. 1a). We set $T = 0$ for our entire model.

The tight-binding Hamiltonian for the central ring of Alice's interferometer is

$$H_R(\phi) = \sum_{n=0}^{N-1} \left[\varepsilon_0 c_n^\dagger c_n + t_0 \left(e^{i\phi/N} c_n^\dagger c_{n+1} + \text{h.c.} \right) \right], \quad (1)$$

with ε_0 and t_0 being the ring's on-site energy and coupling, respectively, and $n + 1$ understood modulo N . Then the retarded Green's function of Alice's interferometer, without coupling to the superconductor, is $\tilde{G}^R(E, \phi) = [E - H(\phi) - \Sigma_{\text{leads}}^R]^{-1}$ where $\Sigma_{\text{leads}}^R = -i(\Gamma^I + \Gamma^{II})/2$ and $(\Gamma^{I,II})_{nm} = \gamma^{I,II} \delta_{nm} \mathbb{1}_{n \in I, II}$ with $\mathbb{1}_{n \in I, II}$ being a rank n identity matrix. The coupling of the superconductor to the ring can be described by the Andreev self-energy diagram [41] shown in Fig. 2, with

$$\Sigma_{AR}^R(E, \phi) = \sum_{i \in \mathcal{S}} \left(\frac{t_{AR} |\Delta|}{g} \right)^2 \tilde{G}_{ii}^R(E, \phi) |i\rangle \langle i|, \quad (2)$$

where \mathcal{S} is the set of sites in the ring coupled to the superconductor, and t_{AR} is the tight-binding coupling between the ring sites and the superconducting sites. Then the *full* retarded Green's function for our model is

$$G^R(E, \phi) = [E - H_R(\phi) - \Sigma^R(E, \phi)]^{-1}, \quad (3)$$

with the full retarded self-energy

$$\Sigma^R(E, \phi) = \Sigma_{\text{leads}}^R + \Sigma_{AR}^R(E, \phi). \quad (4)$$

$$\Sigma_{\text{AR}}^R(a, a; E) = \text{Diagram} \equiv \text{Diagram} \quad (5)$$

FIG. 2. Retarded Andreev self-energy Σ_{AR}^R diagram. The double line in the central figure represents the Cooper pair and the two vertices (crosses) in the figure on the right are the Andreev coefficients $t_{\text{AR}}\Delta/g$.

To quantify decoherence, we compute the transmission function, contrast, and local density of states (LDOS) of Alice's interferometer

$$T(E, \phi) = \text{Tr} [G^I G^R(E, \phi) \Gamma^{II} G^A(E, \phi)], \quad (6)$$

$$C(E, \phi) = \frac{2|T(E, \phi/2) - T(E, 0)|}{T(E, \phi/2) + T(E, 0)}, \quad (7)$$

$$\rho(x, E, \phi) = \langle x | A(E, \phi) | x \rangle, \quad (8)$$

respectively, where $G^A = [G^R]^\dagger$ is the advanced Green's function,

$$A(E, \phi) = \frac{1}{2\pi i} [G^A(E, \phi) - G^R(E, \phi)], \quad (9)$$

is the spectral function, and x is one of the sites in the ring. The transmission function gives the probability that an injected electron reaches the drain, summed over incoming and outgoing channels [42]. The contrast describes how strongly $T(E, \phi)$ oscillates with flux Φ . The LDOS describes how much spectral weight is available at site x [43].

For all of our simulations, we use the fixed preset parameters: $N_{\text{ring}} = 100$, $\phi = \pi$, $\varepsilon_0 = 0$, $t_0 = -1$, $|\Delta| = g = 1$, $\gamma^{I,II} = 0.2$, $\text{rank}=20$ $\Gamma^{I,II}$ matrices, and $\mathcal{S} = \{20, \dots, 29\}$ (so $M_y = |\mathcal{S}| = 10$ superconducting sites).

Decoherence and Reemergence of Coherence—The transmission function T , contrast C , and LDOS ρ are plotted in the limits of weak, intermediate, and strong coupling to the superconductor in Fig. 3, where the green curves show the transmission and contrast without the coupling to the superconductor, and the red curves include the superconductor. In the *weak* coupling regime $0 \leq t_{\text{AR}} \leq 0.3$, the transmission and contrast are suppressed due to Andreev reflection, demonstrating decoherence near the SN interface (see Figs. 3a and 4a). In this regime, the superconductor provides an additional channel that can harvest which-path information (once superconducting degrees of freedom are traced out), thus reducing the contrast.

Interestingly, in the *intermediate* coupling regime $0.4 \leq t_{\text{AR}} \leq 0.6$, Andreev processes start to dominate and the superconductor acts more like a coherent phase-conjugating mirror, resulting in the reemergence of coherence near the SN interface (see Fig. 4b). This is because two successive AR close the detour into a coherent return

channel, so the which-path leakage becomes a reversible virtual process, yielding the return of AB contrast. In the gravitational analogue problem, we speculate that this would correspond to coherent transmission mediated by virtual Hawking radiation.

The *strong* coupling regime $t_{\text{AR}} \geq 2$ shows pronounced subgap spectral features localized along the SN interface. This is directly seen in the LDOS plot of Fig. 3b and schematically in Fig. 1b. These standing waves are associated with a resonant peak in the transmission and contrast. These correspond to proximity-induced Andreev bound states which are coherent electron-hole resonances generated by repeated Andreev conversion [44–51]. In this regime, the real part (Lamb shift) of the Andreev self-energy Σ_{AR}^R pushes the sites along the SN interface away from the band center, leading to reduced AB contrast in the transmission (see LDOS plot of Fig. 3b). Further increases in coupling lead to $T(E, \phi)$ and $C(E, \phi)$ converging to 1 and 0, respectively, signaling that the sites coupled to S are essentially blocked by a very large Lamb shift.

Mathematical Analogy to Gravitation—Recall that the Unruh effect [10–12] is formulated via a Bogoliubov transformation between inertial (Minkowski) and accelerated (Rindler) mode operators, under which the Minkowski vacuum becomes an entangled state across the causally disconnected left and right Rindler wedges [52, 53]. For the Dirac (fermionic) case, this structure is obtained by analytic continuation of positive-frequency ω mode solutions across the Rindler horizon, leading to mode relations that explicitly contain the Unruh factor $e^{-\pi\omega/a}$ [53, 54]. Schematically, the Minkowski vacuum $|0\rangle_{\text{M}}$ may be written as an entangled superposition of excitations built on the Rindler product vacuum $|0_{\text{I}}0_{\text{II}}\rangle$ of the wedge-I $|0_{\text{I}}\rangle$ and wedge-II $|0_{\text{II}}\rangle$ vacua (see Ref. [53, Eq. (160)])

$$|0\rangle_{\text{M}} \propto \prod_{\omega, \mathbf{k}_\perp, n} \left(1 + e^{-\pi\omega/a} c_{\omega, \mathbf{k}_\perp}^{\text{I}, n \dagger} d_{\omega, -\mathbf{k}_\perp}^{\text{II}, \bar{n} \dagger} \right) \times \left(1 - e^{-\pi\omega/a} c_{\omega, \mathbf{k}_\perp}^{\text{II}, n \dagger} d_{\omega, -\mathbf{k}_\perp}^{\text{I}, \bar{n} \dagger} \right) |0_{\text{I}}0_{\text{II}}\rangle. \quad (10)$$

A uniformly accelerated observer restricted to a single wedge therefore describes the Minkowski vacuum by a thermal reduced density operator after tracing over the inaccessible wedge [53, 54].

Strikingly, the same mathematical structure appears in the superconducting case: the BCS ground state $|\text{BCS}\rangle$ is the Bogoliubov vacuum of Bogoliubov-de Gennes (BdG) quasiparticles, but when written in terms of the underlying electron operators it is a paired Gaussian state with a Schmidt-like product structure under an appropriate partition [26, 55]

$$|\text{BCS}\rangle = \prod_{\mathbf{k}} \left(u_{\mathbf{k}} + v_{\mathbf{k}} c_{\mathbf{k}\uparrow}^\dagger c_{-\mathbf{k}\downarrow}^\dagger \right) |0\rangle. \quad (11)$$

A key distinction is that the Nambu doubling reorganizes a single electronic Fock space into particle-hole sectors

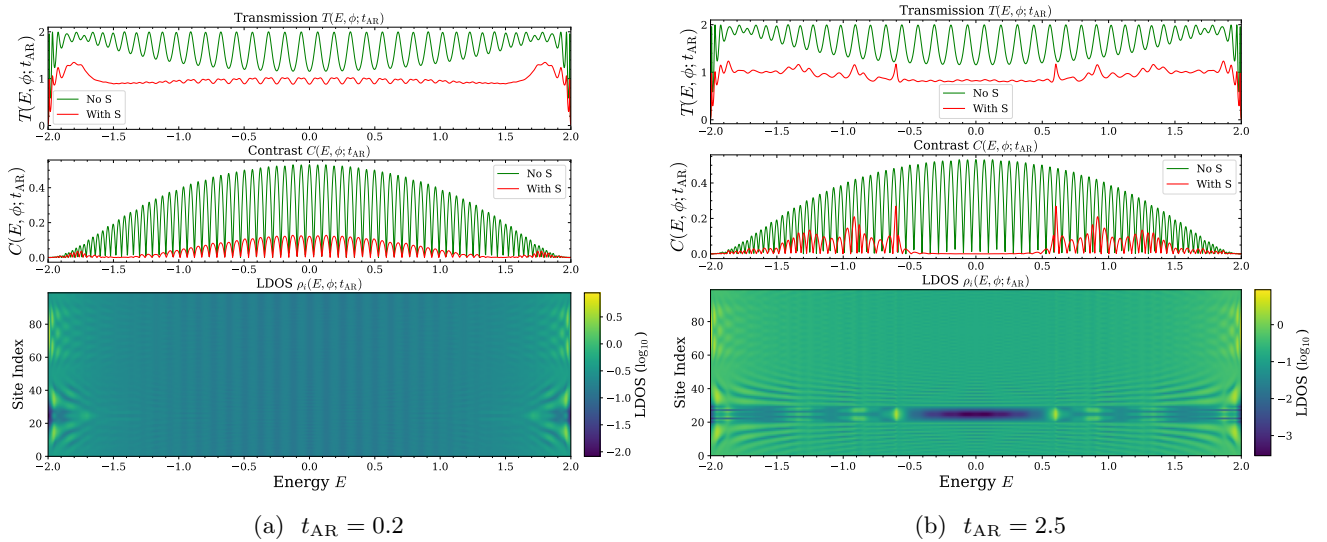


FIG. 3. Transmission $T(E, \phi; t_{AR})$, contrast $C(E, \phi; t_{AR})$, and LDOS $\rho(E, \phi; t_{AR})$ vs energy E for various t_{AR} values with fixed preset parameters: $N_{\text{ring}} = 100$, $(M_x, M_y) = (0, 10)$, $\phi = \pi$, $\varepsilon_0 = \varepsilon_S = 0$, $t_0 = t_x = t_y = t'_x = -1$, $|\Delta| = g = 1$, $\gamma^{I,II} = 0.2$, and $\text{rank}=20$ $\Gamma^{I,II}$ matrices. We observe decoherence in Fig. 3a and the reemergence of coherence in Figs. 3b. See ancillary file for a video illustrating the evolution of T , C , and ρ as a function of t_{AR} .

relative to the Fermi energy E_F , whereas in relativistic Dirac theory, particles/antiparticles are associated with distinct creation/annihilation operators restricted to positive energies. This motivates a unified viewpoint in which “particle content” depends on the chosen mode decomposition, while reduced descriptions obtained by tracing out inaccessible sectors acquire effective thermality.

Importantly, the effective thermality produced by the Bogoliubov mixing in superconductors is generally not exactly thermal. At $T = 0$, tracing over one sector of a paired Gaussian ground state yields a reduced state whose entanglement spectrum is described by a generalized Gibbs ensemble with a mode-dependent reciprocal temperature $\beta_e(\xi)$ [55]. Near the Fermi surface, this can be well approximated by a grand canonical ensemble with $\beta = 2/\Delta$. The associated entanglement entropy obeys an “area law” scaling, $S \propto \pi g(0)\Delta$, and is directly tied to number fluctuations [55].

The connection between the SN model and the Dirac field theory in Rindler space is not a coincidence [56, 57]. At subgap energies near the Fermi surface, $|E - E_F| < \Delta$, Alice’s interferometer is naturally described by the continuum Nambu spinor BdG theory [58, 59] rather than the full microscopic lattice model. In the low-energy limit, i.e. Andreev approximation [33], we can linearize the normal-state dispersion about the Fermi momentum k_F and bundle the electron u and hole v amplitudes into a Nambu spinor $\Psi = (u, v)^T$ [60]. This effectively reduces the Andreev dynamics to a first-order Dirac-like equation

$$i\hbar\partial_t\Psi = [-i\hbar\tau_3\mathbf{v}_F \cdot \nabla + \Re\Delta(\mathbf{x})\tau_1 - \Im\Delta(\mathbf{x})\tau_2]\Psi, \quad (12)$$

where the pairing field $\Delta(\mathbf{x})$ acts as a mass-like term, τ_i are the 2×2 Nambu matrices for $i = 1, 2, 3$, and the electron-hole conversion is encoded by the off-diagonal Bogoliubov mixing [56, 57]. In this sense, the low-energy sector of the SN system has the same spinor-field structure as the Dirac field theory in Rindler space, with the condensed matter doubling being a Nambu particle-hole doubling relative to E_F rather than the particle-antiparticle doubling of relativistic QFT.

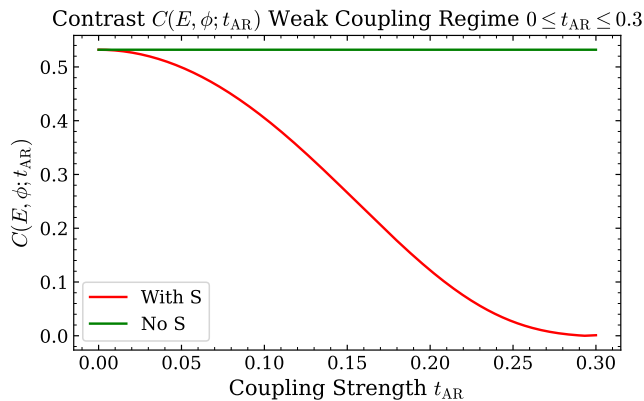
Distance Dependence of Decoherence Rate—To calculate the distance dependence of the SS-DSW decoherence, we introduce a 2D normal metal spacer between the N -ring and S with M_x horizontal and M_y vertical sites, giving a total of $M_x M_y$ sites (see Fig. 1a, details given in Appendix A).

To quantify the spatial dependence of the decoherence rate, we utilize the transport-weighted [61] dephasing rate

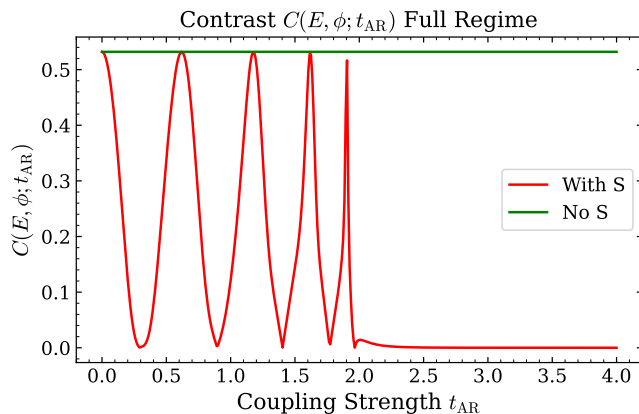
$$\frac{\Gamma_\phi(E, \phi)}{\hbar} = -\frac{2\text{Tr}[\Sigma_{AR}^R(E)G^R(E, \phi)\Gamma^I G^A(E, \phi)]}{\hbar\text{Tr}[G^R(E, \phi)\Gamma^I G^A(E, \phi)]}. \quad (13)$$

Eq. (13) gives the effective rate at which the SN coupling t_{AR} destroys phase information [61].

We see in Fig. (5a) that for multiple S sites on the spacer, the dephasing $\Gamma_\phi(E, \phi; M_x)$ as a function of M_x exhibits an approximate $1/M_x$ ($1/r$) trend. The spread among the different M_y curves is a finite-size quantum size effect where the discrete mesoscopic spacer geometry modifies the interference pattern, producing geometry-dependent oscillations around the same decaying envelope. To suppress these quantum size fluctuations, we average over various S sites in Fig. 5b and find that the



(a)



(b)

FIG. 4. Contrast $C(E, \phi; t_{\text{AR}})$ as a function of t_{AR} . (a) We see contrast suppression in the weak coupling regime until $t_{\text{AR}} = 0.3$. (b) We see the oscillatory behavior of the reemergence of coherence until the final contrast suppression in the strong coupling regime. We use the fixed preset parameters: $N_{\text{ring}} = 100$, $E = 0$, $\phi = \pi$, $t_{\text{AR}} = 0.2$, $\varepsilon_0 = \varepsilon_S = 0$, $t_0 = t_x = t_y = t'_x = -1$, $|\Delta| = g = 1$, $\gamma^{I,II} = 0.2$, and $\text{rank}=20$ $\Gamma^{I,II}$ matrices.

M_y -averaged dephasing $\bar{\Gamma}_\phi(E, \phi; M_x)$ exhibits an approximate $1/M_x$ ($1/r$) trend, in qualitative agreement with the DSW decoherence scaling of $1/r^3$ [1, 29–31]. We note that the original DSW decoherence scaling arises in a three-dimensional geometry, whereas our model is effectively one-dimensional, so the corresponding distance dependence is naturally weaker.

In the SN structure, Δ plays the role of an effective horizon for subgap modes: there are no propagating quasiparticle excitations in S for $|E| < \Delta$ at $T = 0$, while the influence of S on N is confined to a proximity layer of thickness $\xi \sim \hbar v_F / \Delta$ (the superconducting coherence length), which shrinks as $\Delta \rightarrow \infty$ [32]. In this limit, a probe restricted to the normal region at distances $x \gg \xi$ effectively accesses only the reduced state of N, while subgap transport is governed by Andreev re-

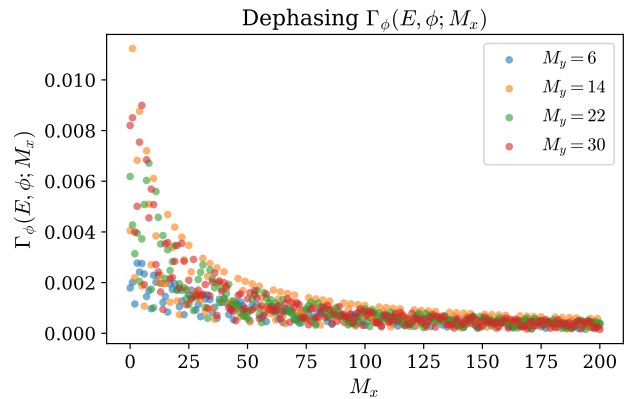
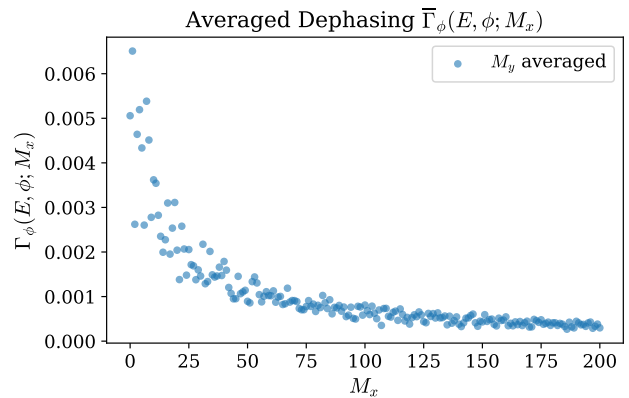
(a) $M_y \in \{6, 14, 22, 30\}$ (b) Averaged over $M_y \in \{6, 14, 22, 30\}$

FIG. 5. Dephasing $\Gamma_\phi(E, \phi; M_x)$ vs horizontal sites M_x for weak coupling $t_{\text{AR}} = 0.2$. The dephasing exhibits an approximate $1/M_x$ ($1/r$) trend. We use the fixed preset parameters: $N_{\text{ring}} = 100$, $E = 0$, $\phi = \pi$, $t_{\text{AR}} = 0.2$, $\varepsilon_0 = \varepsilon_S = 0$, $t_0 = t_x = t_y = t'_x = -1$, $|\Delta| = g = 1$, $\gamma^{I,II} = 0.2$, and $\text{rank}=20$ $\Gamma^{I,II}$ matrices.

flection, which implements electron-hole Bogoliubov mixing. In this sense, the proximity region plays the role of an analogue near-horizon (Rindler-like) region, while the gapped superconducting sector acts as the analogue black hole interior.

Discussion—We have demonstrated a solid-state analogue of the DSW decoherence in a superconductor-normal metal AB interferometer. At weak SN coupling t_{AR} , Andreev processes suppress the interference contrast, providing a condensed matter analogue of horizon-induced decoherence. In an interesting twist, we found a reemergence of coherence at intermediate coupling, which we interpret as due to resonant tunneling through Andreev bound states. In the spacer model, the transport-weighted dephasing exhibited an approximate $1/M_x$ ($1/r$) decay after averaging over quantum size fluctuations, consistent with the weaker distance dependence

expected for an effectively one-dimensional analogue of the gravitational problem.

Our results support a unified horizon analogy in which the superconducting gap defines an effective inaccessible sector, Andreev reflection plays the role of Hawking radiation, and the low-energy (near Fermi surface) effective field theory takes on a Dirac-like Nambu spinor form. Beyond merely theoretical interest, this one-to-one conceptual mapping opens the possibility of leveraging superconducting interferometers as experimental platforms for studying decoherence from horizon-like physics. Given the ubiquity of Hawking-like radiation in various analog systems, we hypothesize that similar analogue DSW decoherence could exist in other analogue platforms. On

a speculative level, our results suggest that coherence restoration mediated by virtual Hawking radiation may also be possible for real black holes. If so, such a mechanism would indicate that horizon-induced decoherence need not be strictly monotonic, and that some phase information could in principle be reencoded in quantum fluctuations on the exterior of the horizon. While it seems that this suggests information recovery, it would not on its own resolve the black hole information loss problem.

Acknowledgments—We thank Sam Gralla, Morifumi Mizuno, Parth Kumar, Marco A Jimenez-Valencia, Anand Natarajan, and Xingzhou Yu for the helpful comments and discussions in the formulation of this work.

-
- [1] D. L. Danielson, G. Satishchandran, and R. M. Wald, Black holes decohere quantum superpositions, *International Journal of Modern Physics D* **31**, 2241003 (2022).
- [2] S. K. Manikandan and A. N. Jordan, Andreev reflections and the quantum physics of black holes, *Physical Review D* **96**, 124011 (2017).
- [3] C. Barceló, S. Liberati, and M. Visser, Analogue Gravity, *Living Reviews in Relativity* **14**, 3 (2011).
- [4] W. G. Unruh, Experimental Black-Hole Evaporation?, *Physical Review Letters* **46**, 1351 (1981).
- [5] W. G. Unruh, Sonic analogue of black holes and the effects of high frequencies on black hole evaporation, *Physical Review D* **51**, 2827 (1995).
- [6] G. E. Volovik, Superfluid $^3\text{He-B}$ and gravity, *Physica B: Condensed Matter* **162**, 222 (1990).
- [7] G. E. Volovik and K. Zhang, Lifshitz Transitions, Type-II Dirac and Weyl Fermions, Event Horizon and All That, *Journal of Low Temperature Physics* **189**, 276 (2017).
- [8] S. W. Hawking, Particle creation by black holes, *Communications In Mathematical Physics* **43**, 199 (1975).
- [9] S. W. Hawking, Breakdown of predictability in gravitational collapse, *Physical Review D* **14**, 2460 (1976).
- [10] S. A. Fulling, Nonuniqueness of Canonical Field Quantization in Riemannian Space-Time, *Physical Review D* **7**, 2850 (1973).
- [11] P. C. W. Davies, Scalar production in Schwarzschild and Rindler metrics, *Journal of Physics A: Mathematical and General* **8**, 609 (1975).
- [12] W. G. Unruh, Notes on black-hole evaporation, *Physical Review D* **14**, 870 (1976).
- [13] G. E. Volovik, Simulation of a Panlevé-Gullstrand black hole in a thin $^3\text{He-A}$ film, *Journal of Experimental and Theoretical Physics Letters* **69**, 705 (1999).
- [14] U. R. Fischer and G. E. Volovik, Thermal quasi-equilibrium states across Landau horizons in the effective gravity of superfluids, *International Journal of Modern Physics D* **10**, 57 (2001).
- [15] C. Barceló, S. Liberati, and M. Visser, Analogue gravity from Bose-Einstein condensates, *Classical and Quantum Gravity* **18**, 1137 (2001).
- [16] S. K. Manikandan and A. N. Jordan, Bosons falling into a black hole: A superfluid analogue, *Physical Review D* **98**, 124043 (2018).
- [17] G. E. Volovik, Black hole and Hawking radiation by type-II Weyl fermions, *JETP Letters* **104**, 645 (2016).
- [18] E. Bilokon, V. Bilokon, F. Großmann, J. R. Williams, and D. I. Bondar, Hilbert Space Black Hole Analogue: Unidirectional Transport without Driving (2026), arXiv:2602.20508 [quant-ph].
- [19] J. Steinhauer, Observation of quantum Hawking radiation and its entanglement in an analogue black hole, *Nature Physics* **12**, 959 (2016).
- [20] J. R. Muñoz de Nova, K. Golubkov, V. I. Kolobov, and J. Steinhauer, Observation of thermal Hawking radiation and its temperature in an analogue black hole, *Nature* **569**, 688 (2019).
- [21] V. I. Kolobov, K. Golubkov, J. R. Muñoz de Nova, and J. Steinhauer, Observation of stationary spontaneous Hawking radiation and the time evolution of an analogue black hole, *Nature Physics* **17**, 362 (2021).
- [22] A. Fabbri and R. Balbinot, Ramp-up of Hawking Radiation in Bose-Einstein-Condensate Analog Black Holes, *Physical Review Letters* **126**, 111301 (2021).
- [23] J. Steinhauer, Observation of self-amplifying Hawking radiation in an analogue black-hole laser, *Nature Physics* **10**, 864 (2014).
- [24] J. Drori, Y. Rosenberg, D. Bermudez, Y. Silberberg, and U. Leonhardt, Observation of Stimulated Hawking Radiation in an Optical Analogue, *Physical Review Letters* **122**, 010404 (2019).
- [25] P. D. Nation, M. P. Blencowe, A. J. Rimberg, and E. Buks, Analogue Hawking Radiation in a dc-SQUID Array Transmission Line, *Physical Review Letters* **103**, 087004 (2009).
- [26] J. Bardeen, L. N. Cooper, and J. R. Schrieffer, Theory of Superconductivity, *Physical Review* **108**, 1175 (1957).
- [27] T. Jacobson, On the origin of the outgoing black hole modes, *Physical Review D* **53**, 7082 (1996).
- [28] S. K. Manikandan and A. N. Jordan, Black holes as Andreev reflecting mirrors, *Physical Review D* **102**, 064028 (2020).
- [29] D. L. Danielson, G. Satishchandran, and R. M. Wald, Killing horizons decohere quantum superpositions, *Physical Review D* **108**, 025007 (2023).
- [30] D. L. Danielson, G. Satishchandran, and R. M. Wald, Local description of decoherence of quantum superpositions by black holes and other bodies, *Physical Review D* **111**, 025014 (2025).

- [31] S. E. Gralla and H. Wei, Decoherence from horizons: General formulation and rotating black holes, *Physical Review D* **109**, 065031 (2024).
- [32] G. E. Blonder, M. Tinkham, and T. M. Klapwijk, Transition from metallic to tunneling regimes in superconducting microconstrictions: Excess current, charge imbalance, and supercurrent conversion, *Physical Review B* **25**, 4515 (1982).
- [33] A. F. Andreev, The thermal conductivity of the intermediate state in superconductors, *Sov. Phys. JETP* **19**, 1228 (1964).
- [34] B. Pannetier and H. Courtois, Andreev Reflection and Proximity effect, *Journal of Low Temperature Physics* **118**, 599 (2000).
- [35] C. W. J. Beenakker, Specular Andreev Reflection in Graphene, *Physical Review Letters* **97**, 067007 (2006).
- [36] C. W. J. Beenakker, Colloquium: Andreev reflection and Klein tunneling in graphene, *Reviews of Modern Physics* **80**, 1337 (2008).
- [37] Z. Hou and Q.-F. Sun, Double Andreev reflections in type-II Weyl semimetal-superconductor junctions, *Physical Review B* **96**, 155305 (2017).
- [38] Y. Aharonov and D. Bohm, Significance of Electromagnetic Potentials in the Quantum Theory, *Physical Review* **115**, 485 (1959).
- [39] R. A. Webb, S. Washburn, C. P. Umbach, and R. B. Laibowitz, Observation of $\frac{h}{e}$ Aharonov-Bohm Oscillations in Normal-Metal Rings, *Physical Review Letters* **54**, 2696 (1985).
- [40] S. Olariu and I. I. Popescu, The quantum effects of electromagnetic fluxes, *Reviews of Modern Physics* **57**, 339 (1985).
- [41] P. Coleman, *Introduction to Many Body Physics*, 1st ed. (Cambridge University Press, Cambridge, 2008).
- [42] S. Datta, *Electronic Transport in Mesoscopic Systems*, Cambridge Studies in Semiconductor Physics and Microelectronic Engineering (Cambridge University Press, Cambridge, 1995).
- [43] G. Stefanucci and R. van Leeuwen, *Nonequilibrium Many-Body Theory of Quantum Systems*, 2nd ed. (Cambridge University Press, Cambridge, 2025).
- [44] A. F. Andreev, Electron spectrum of the intermediate state of superconductors, *Zhurnal Eksperimental'noi i Teoreticheskoi Fiziki (U.S.S.R.)* For English translation see *Sov. Phys. - JETP (Engl. Transl.)* **49**, 455 (1965).
- [45] I. O. Kulik, Macroscopic Quantization and the Proximity Effect in S-N-S Junctions, *Soviet Journal of Experimental and Theoretical Physics* **30**, 944 (1969).
- [46] C. W. J. Beenakker, Quantum transport in semiconductor-superconductor microjunctions, *Physical Review B* **46**, 12841 (1992).
- [47] I. K. Marmoros, C. W. J. Beenakker, and R. A. Jalabert, Three signatures of phase-coherent Andreev reflection, *Physical Review B* **48**, 2811 (1993).
- [48] K.-M. H. Lenssen, M. R. Leys, and J. H. Wolter, Experimental signature of phase-coherent Andreev reflection, *Physical Review B* **58**, 4888 (1998).
- [49] L. Bretheau, Ç. Ö. Girit, H. Pothier, D. Esteve, and C. Urbina, Exciting Andreev pairs in a superconducting atomic contact, *Nature* **499**, 312 (2013).
- [50] J. A. Sauls, Andreev bound states and their signatures, *Philosophical Transactions of the Royal Society A: Mathematical, Physical and Engineering Sciences* **376**, 20180140 (2018).
- [51] M. Hays, G. de Lange, K. Serniak, D. J. van Woerkom, D. Bouman, P. Krogstrup, J. Nygård, A. Geresdi, and M. H. Devoret, Direct Microwave Measurement of Andreev-Bound-State Dynamics in a Semiconductor-Nanowire Josephson Junction, *Physical Review Letters* **121**, 047001 (2018).
- [52] L. C. B. Crispino, A. Higuchi, and G. E. A. Matsas, The Unruh effect and its applications, *Reviews of Modern Physics* **80**, 787 (2008), arXiv:0710.5373 [gr-qc, physics:hep-th].
- [53] K. Ueda, A. Higuchi, K. Yamamoto, A. Rohim, and Y. Nan, Entanglement of the vacuum between left, right, future, and past: Dirac spinor in Rindler and Kasner spaces, *Physical Review D* **103**, 125005 (2021).
- [54] M. Soffel, B. Müller, and W. Greiner, Dirac particles in Rindler space, *Physical Review D* **22**, 1935 (1980).
- [55] X. M. Puspus, K. H. Villegas, and F. N. C. Paraan, Entanglement spectrum and number fluctuations in the spin-partitioned BCS ground state, *Physical Review B* **90**, 155123 (2014).
- [56] G. E. Volovik, Superfluid analogies of cosmological phenomena, *Physics Reports* **351**, 195 (2001).
- [57] G. E. Volovik, *The Universe in a Helium Droplet* (OUP Oxford, 2003).
- [58] N. N. Bogolyubov, On the theory of superfluidity, *J. Phys. (USSR)* **11**, 23 (1947).
- [59] P. G. D. Gennes, *Superconductivity Of Metals And Alloys* (CRC Press, Boca Raton, 2018).
- [60] Y. Nambu, Quasi-Particles and Gauge Invariance in the Theory of Superconductivity, *Physical Review* **117**, 648 (1960).
- [61] C. A. Stafford, Local temperature of an interacting quantum system far from equilibrium, *Physical Review B* **93**, 245403 (2016).

Appendix A: Normal Metal Spacer Tight-Binding Hamiltonian

The 2D normal metal spacer's tight-binding Hamiltonian H_N is

$$H_N = H_N^{\text{on}} + H_N^{(x)} + H_N^{(y)}, \quad (\text{A1})$$

$$H_N^{\text{on}} = \varepsilon_S \sum_{n,m=0}^{M_x-1, M_y-1} c_{j(n,m)}^\dagger c_{j(n,m)}, \quad (\text{A2})$$

$$H_N^{(x)} = t_x \sum_{n,m=0}^{M_x-2, M_y-1} \left(c_{j(n,m)}^\dagger c_{j(n+1,m)} + \text{h.c.} \right), \quad (\text{A3})$$

$$H_N^{(y)} = t_y \sum_{n,m=0}^{M_x-1, M_y-2} \left(c_{j(n,m)}^\dagger c_{j(n,m+1)} + \text{h.c.} \right), \quad (\text{A4})$$

where $n = 0, 1, \dots, M_x - 1$, $m = 0, 1, \dots, M_y - 1$, and $j(n, m) = N + (n - 1)M_y + m$. The spacer-ring tight-binding Hamiltonian is

$$H_{\text{N-R}} = t'_x \sum_{m=0}^{M_y-1} \left(c_{r_m}^\dagger c_{j(0,m)} + \text{h.c.} \right), \quad (\text{A5})$$

where r_n is the n -th ring site of the coupling between the ring and the spacer with t'_x being the coupling of the spacer and ring.

Appendix B: Mathematical Connection Between the Low-Energy BdG Theory and Dirac Field Theory

At subgap energies close to the Fermi surface $|E - E_F| < \Delta$, the physics of the SN system are governed by the 2×2 Bogoliubov-de Gennes (BdG) equations [58, 59]

$$H_{\text{BdG}} \psi(\mathbf{x}) = E \psi(\mathbf{x}), \quad (\text{B1})$$

$$H_{\text{BdG}} = \begin{pmatrix} H_0 & \Delta(\mathbf{x}, t) \\ \bar{\Delta}(\mathbf{x}, t) & -H_0 \end{pmatrix}, \quad (\text{B2})$$

$$\psi(\mathbf{x}, t) = \begin{pmatrix} u(\mathbf{x}, t) \\ v(\mathbf{x}, t) \end{pmatrix}, \quad (\text{B3})$$

$$H_0 = -\frac{\hbar^2}{2m} \nabla_\perp^2 - \mu(\mathbf{x}) + V(\mathbf{x}) = -\frac{\hbar^2}{2m} (\partial_x^2 + \partial_y^2) - \mu(\mathbf{x}) + V(\mathbf{x}), \quad (\text{B4})$$

$$\Delta(\mathbf{x}, t) = \Delta_0(\mathbf{x}, t) e^{i\phi_S(\mathbf{x}, t)}, \quad (\text{B5})$$

where $\mu(\mathbf{x})$ is the chemical potential. Note that we have promoted the gap $\Delta(\mathbf{x}, t)$ to be time and space-dependent. Observe that we can decompose the gap $\Delta(\mathbf{x}, t)$ as

$$\Delta(\mathbf{x}, t) = \Delta_1(\mathbf{x}, t) + i\Delta_2(\mathbf{x}, t), \quad \bar{\Delta}(\mathbf{x}, t) = \Delta_1(\mathbf{x}, t) - i\Delta_2(\mathbf{x}, t), \quad (\text{B6})$$

where

$$\Delta_1(\mathbf{x}, t) = \Re(\Delta(\mathbf{x}, t)) = \Delta_0(\mathbf{x}, t) \cos(\phi_S(\mathbf{x}, t)), \quad (\text{B7})$$

$$\Delta_2(\mathbf{x}, t) = \Im(\Delta(\mathbf{x}, t)) = \Delta_0(\mathbf{x}, t) \sin(\phi_S(\mathbf{x}, t)). \quad (\text{B8})$$

Then Hamiltonian (B2) can be written as

$$H_{\text{BdG}} = \vec{h} \cdot \vec{\tau} = H_0 \tau_3 + \Delta_1(\mathbf{x}, t) \tau_1 - \Delta_2(\mathbf{x}, t) \tau_2, \quad (\text{B9})$$

where

$$\vec{h} = (\Delta_1(\mathbf{x}, t), -\Delta_2(\mathbf{x}, t), H_0), \quad (\text{B10})$$

$$\vec{\tau} = (\tau_1, \tau_2, \tau_3) = \left(\begin{pmatrix} 0 & 1 \\ 1 & 0 \end{pmatrix}, \begin{pmatrix} 0 & -i \\ i & 0 \end{pmatrix}, \begin{pmatrix} 1 & 0 \\ 0 & -1 \end{pmatrix} \right) \quad (\text{B11})$$

are the Hamiltonian vector and 2×2 Nambu matrices, respectively. Note that the Nambu matrices $\vec{\tau}$ are the Pauli matrices except that they act on Nambu space.

Suppose that the chemical potential is constant with a value of $\mu = \hbar^2 k_F^2 / (2m)$. Without loss of generality, we let the potential energy V be constant and set to $V = 0$. If $V \neq 0$, then V can be absorbed into the ground state energy. Then we have the simplification

$$H_0 = -\frac{\hbar^2}{2m} \nabla_{\perp}^2 - \mu. \quad (\text{B12})$$

To study Andreev reflection, we work under the Andreev approximation where $E \ll \Delta(\mathbf{x}, t)$ and assume that $\Delta(\mathbf{x}, t)$ varies slowly over scales of order k_F^{-1} [33]. Now we use the following Ansatz for the two-components of the Nambu spinor ψ

$$u(\mathbf{x}, t) = f(\mathbf{x}, t) e^{i\mathbf{k}_F \cdot \mathbf{x}}, \quad (\text{B13})$$

$$v(\mathbf{x}, t) = g(\mathbf{x}, t) e^{i\mathbf{k}_F \cdot \mathbf{x}}, \quad (\text{B14})$$

where $\mathbf{k}_F = k_F \hat{\mathbf{k}}_F$ is Fermi wave vector and f and g vary on the scale of k_F^{-1} as well. If we insert Eqs. (B13) and (B14) into Eq. (B1) and ignore terms involving derivatives higher than one, we get the linearized equations [33]

$$-i\hbar \mathbf{v}_F \cdot \nabla_{\perp} f(\mathbf{x}, t) + \Delta(\mathbf{x}, t) g(\mathbf{x}, t) = i\hbar \frac{\partial}{\partial t} f(\mathbf{x}, t), \quad (\text{B15})$$

$$i\hbar \mathbf{v}_F \cdot \nabla_{\perp} g(\mathbf{x}, t) + \bar{\Delta}(\mathbf{x}, t) f(\mathbf{x}, t) = i\hbar \frac{\partial}{\partial t} g(\mathbf{x}, t), \quad (\text{B16})$$

where $\mathbf{v}_F = (\hbar/m)\mathbf{k}_F$ is the Fermi velocity. This yields the linearized BdG Hamiltonian

$$\tilde{H}_{\text{BdG}} = -i\hbar \tau_3 \mathbf{v}_F \cdot \nabla_{\perp} + \Delta_1(\mathbf{x}, t) \tau_1 + \Delta_2(\mathbf{x}, t) \tau_2. \quad (\text{B17})$$

To express the linearized BdG Hamiltonian (B17) in a more mathematically appealing way, we first rewrite the gap terms as

$$\Delta_1(\mathbf{x}, t) \tau_1 + \Delta_2(\mathbf{x}, t) \tau_2 = \Delta_0(\mathbf{x}, t) [\cos(\phi_S(\mathbf{x}, t)) \tau_1 - \sin(\phi_S(\mathbf{x}, t)) \tau_2] = \vec{\Delta}(\mathbf{x}, t) \cdot \vec{\tau}, \quad (\text{B18})$$

where

$$\vec{\Delta}(\mathbf{x}, t) = \Delta_0(\mathbf{x}, t) (\cos(\phi_S(\mathbf{x}, t)), -\sin(\phi_S(\mathbf{x}, t)), 0). \quad (\text{B19})$$

This turns Eq. (B17) into

$$\tilde{H}_{\text{BdG}} = -i\hbar \tau_3 \mathbf{v}_F \cdot \nabla_{\perp} + \vec{\Delta}(\mathbf{x}, t) \cdot \vec{\tau}. \quad (\text{B20})$$

We note that the linearized BdG Hamiltonian (B20) now closely resembles the Dirac equation except that we have a vector-valued effective ‘‘mass’’ term $\vec{\Delta}(\mathbf{x}, t)$ that is position and time-dependent. In addition, the effective mass $\vec{\Delta}(\mathbf{x}, t)$ rotates in Nambu (pseudospin) space as the order parameter $\phi_S(\mathbf{x}, t)$ varies.